RIELAC, Vol. 41 3/2020 p. 41-52 Septiembre-Diciembre ISSN: 1815-5928

RIELAC
Revista de Ingeniería Electrónica, Automática y Comunicaciones

RF modulator upgrading for an NMR spectrometer

Joaquin Enrique Hing Batista, Alejandro Bordelois Boizán, Manuel Ernesto Noda Guerra

ABSTRACT / *RESUMEN*

Low field magnetic resonance (MR) for the study of chemical compounds is a very common and important area of research. However, the greater the intensity of the magnetic field, the better the signal-to-noise ratio of the signal obtained from the substance under study and, therefore, the greater the possibilities of identifying the different chemical compounds. To conduct these studies, an MR spectrometer was built at the Centro de Biofísica Médica (Biophysics and Medical Physics Center), the parts of which were taken from other equipment in the laboratory or modified, such as the radio frequency (RF) modulator. This paper describes the changes and improvements made to the RF modulator that allowed the spectrometer to function correctly at the new 1.5 T field. The aforementioned changes included: changing the modulator's working frequencies to make it work well at the new 64 MHz, change of frequency, changing the RF switch to achieve better attenuation of the non-desired RF signal, designing and implementing a RF switch control circuit and designing and implementing a new 64 MHz passband filter. The performance of the upgraded modulator was demonstrated by measuring harmonic suppression, sideband rejection and conversion loss. Finally, the modulator fitted into the spectrometer was validated by carrying out a complete experiment that ended with the acquisition of an MR signal.

Keywords: Magnetic Resonance, modulator, NMR spectrometer, switch, filter.

La Resonancia Magnética (RM) de bajos campos para el estudio de compuestos químicos es un área muy importante y común de la investigación. Sin embargo, mientras mayor es la intensidad del campo magnético, mejor es la relación señal a ruido de la señal que se obtiene de la sustancia en estudio y, por lo tanto, mayores las posibilidades de identificación de los diferentes compuestos químicos. Para realizar estos estudios se construyó en el Centro de Biofísica Médica un espectrómetro de RM cuyas partes se adquirieron de otros equipos en el laboratorio o se modificaron, como por ejemplo, el modulador de radio frecuencia (RF). En este trabajo se describen los cambios y mejoras realizadas al modulador de RF que permitieron al espectrómetro funcionar correctamente en el nuevo campo de 1,5 T. Los cambios anteriores incluyeron: cambio de las frecuencias de trabajo del modulador para poder operar bien a la nueva frecuencia de 64 MHz, cambio del interruptor de RF para lograr una mejor atenuación de la señal de RF no deseada, diseño e implementación de un circuito controlador del interruptor de RF y diseño e implementación de un nuevo filtro pasabanda a 64 MHz. El rendimiento del modulador modernizado se demostró midiendo la supresión armónica, el rechazo de la banda lateral y la pérdida de conversión. Finalmente se validó el modulador incorporado al espectrómetro mediante la realización de un experimento completo que culminó con la adquisición de una señal de RM.

Palabras claves: Resonancia Magnética, modulador, espectrómetro de RMN, interruptor, filtro.

Título: Modernización de un modulador de RF para un espectrómetro de RMN.

1. INTRODUCTION

Nuclear magnetic resonance (NMR) spectroscopy is a powerful tool for elucidating the molecular chemical structure of organic compounds, with a wide application in biotechnology, medicine, the pharmaceutical medical industry, the food industry, among other branches of science and industry [1-6]. Any NMR experiment consists of placing the spin system under

Recibido: 3/3/2020 Aceptado: 4/8/2020

the action of an external static magnetic field B_0, capable of aligning spins in its direction, determining the appearance of a resulting non-zero magnetization. The sense of orientation can occur in two possible states: one of low energy (parallel) and the other of high energy (anti-parallel).

The application of the RF pulse results in a net absorption, and the energy difference between the spin states parallel to B_0 (which determines absorption intensity) depends on B_0 intensity and the gyromagnetic ratio of the nucleus [1].

The signal-to-noise ratio (SNR), signal resolution and NMR spectra are parameters that vary proportionally with the intensity of the B_0 magnetic field [7-12]. The latter facts are among the reasons why modern spectrometers have increased their magnetic field from very low fields up to very high fields, reaching even 20 T [11-20]. In order to conduct studies of the molecular chemical structure of organic compounds of interest to the Biophysics and Medical Physics Center (CBM) and to compare the results with MRI imaging studies conducted on 1.5 T machines, the need arises for developing an NMR spectrometer at this B_0 intensity (64 MHz); considering that commercial equipment using this technology is extremely expensive due to the use of ultra-high magnetic fields and highly specialized components. Taking from our laboratory different NMR subsystems which worked at 4 MHz and which could be electronically adjusted to 64 MHz, our research team built a functional MR spectrometer, without major technological complications, see Fig. 1.

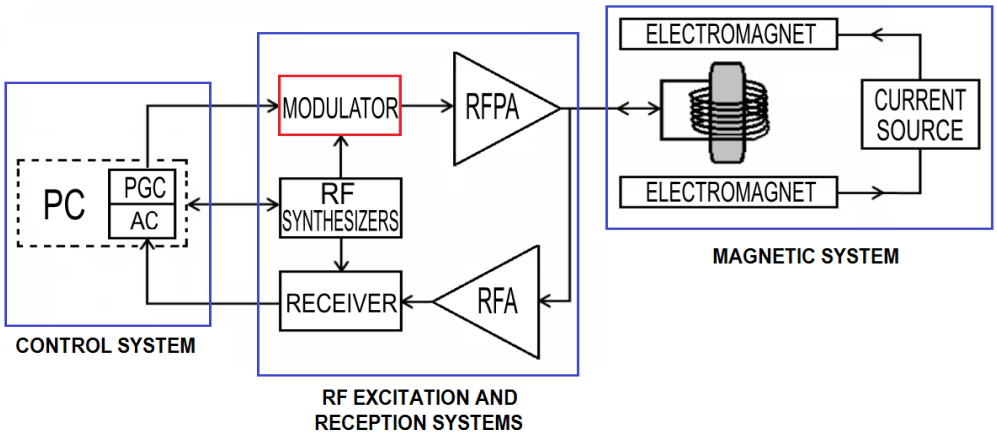

Figure 1

General block diagram of the 64 MHz spectrometer.

In Fig. 1, the Control System consists of a personal computer (PC) with a Pulse Generator Card (PGC) that generates the desired types of excitation pulses and the Acquisition Card (AC). The RF Excitation System includes the PGC, the modulator and the RF power amplifier, and the Reception System consists of a RF preamplifier, the Receiver and the AC. The Magnetic System comprises the current source, the electromagnet and the probehead.

This paper aims at presenting the steps taken to upgrade the RF modulator, which is a key element in the proper functioning of the RF system. The modulator was originally designed to operate at a working frequency of 4 MHz; therefore, it was essential to take several steps to make it function correctly at 64 MHz. The correct performance of the modulator is demonstrated by measuring its parameters in each stage, as well as through the MR signal acquired in a sample of choline dissolved in pure H_2O.

The development of the 64 MHz spectrometer, as well as the upgrading of its RF modulator, changed the goal of the experimental station, from the original NRM images to NMR spectroscopy, and their applications. In addition, it became a teaching basis for learning in NMR technology, since our institution is located in the Universidad de Oriente (University of Oriente).

To present the changes made into the modulator, the document is organized as follows: Section 2, Materials and methods, describes the steps taken to upgrade the modulator and all the aspects associated with each stage; Section 3, Results and discussion, presents the significant results obtained from the measurement of the modulator's updated parameters, as well as the discussion of results to assess the quality and good performance of the modulator. Conclusions and ideas for future work are presented in Section 4.

2.- MATERIALS AND METHODS

To achieve a field of 1.5 T in the spectrometer of Fig. 1 a high stability current source was set up with 54 A approximately, feeding a 0.58 Ω electromagnet. The spectrometer is controlled by the PC, the PGC that indicates the types of pulses desired and the AC that processes the signal coming from the receiver channel. The RF Excitation Systems consists of the PCI-766 pulse generator card, the modulator that modulates the signal coming from the synthesizers, and the RF Power Amplifier AN8063. On the other hand, the Reception channel is composed of the RF Preamplifier (RFA) AU-2A, the receiver that translates the signal from 64 MHz to baseband and then filters it, and finally the PCI-730 acquisition card. The latter card is also used to digitally control the modulator and RF power amplifier. In both channels, the synthesizer NOVATEC DDS7 (frequency output of 10 MHz) and PM5192 (frequency output of 74 MHz) are used.

2.1.- THE MODULATOR

To upgrade the modulator, the following actions were performed:

1- Changing the frequencies, the modulator needs to work properly at 64 MHz.

2- Checking that all components inside the modulator can operate well at the desired frequencies.

3- Checking the performance of the RF switch to attenuate the output signal when required (and design one if necessary).

4- Building and changing the filter at the output of the modulator.

5- Validating the modulator performance.

To carry out the above steps, the following software and tools were employed: the design of all schematic circuits and their simulations were implemented using the KiCad software tool, and the graphs shown in this paper were made on the OCTAVE software. The characterization of the filter was made employing the Agilent N9923A network analyser. The acquisition and measurement of the modulator data was made using the TEKTRONIX TBS1154 digital oscilloscope.

2.1.1- SETTING UP THE FREQUENCIES OF THE MODULATOR

The first task in upgrading the modulator was to change the frequencies it works with. These frequencies will be called the working frequency, the intermediate frequency and the synthesizer frequency. The upgraded modulator along with all its signals and components are shown in Fig. 2.

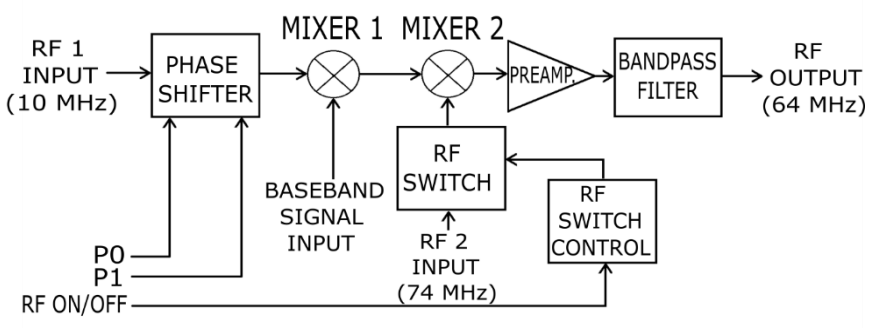

Figure 2

Scheme of the new upgraded modulator (with new signal frequencies at RF 1 INPUT, RF 2 INPUT and RF OUTPUT ports, new circuits at RF SWITCH, RF SWITCH CONTROL and PASSBAND FILTER modules).

The working frequency (signal at RF OUTPUT in Fig. 2) is the frequency needed to perturb the net magnetization in an NMR experiment and once the main magnetic field is fixed, it can be calculated using the Larmor equation (1) [9].

$$\omega_0 = \gamma B_0 \quad (1)$$

where γ is the gyromagnetic constant (42,57 MHz/T for ^1H), B_0 is the magnetic field intensity of the electromagnet (T) and ω_0 is precession frequency (Hz). For this work, B_0 must be substituted by 1.5 T, and equation (1) yields a working frequency of 64 MHz; therefore, this is the frequency that must be achieved at the output of the modulator to properly excite the net magnetization at 1.5 T.

The intermediate frequency (signal at RF 1 INPUT in Fig. 2) allows working in a lower frequency and helps to obtain, through mixing, the working frequency. This frequency was set up to 10 MHz in the old modulator and is kept at this value in this upgraded version.

The synthesizer frequency (signal at RF 2 INPUT in Fig. 2) is the other stable high frequency signal that allows to obtain, through mixing, the working frequency. In order to obtain the 64 MHz working frequency mentioned above, the synthesizer frequency is fixed at 74 MHz. This 74 MHz signal mixed with 10 MHz yields, among other results, the difference frequency (74 MHz - 10 MHz = 64 MHz), which is the working frequency desired.

The baseband signal is the envelope of the RF pulse necessary to excite the probe. It is generated in the PC (Fig.1) and enters the modulator through BASEBAND SIGNAL INPUT port in Fig. 2. It may be gaussian, squared or sinc (sin(x)/x).

The general operation of the modulator (Fig. 2) is described as follows: The 10 MHz intermediate signal at RF 1 INPUT port enters to PHASE SHIFTER module and is shifted by 0, 90, 180 and 270 degrees as selected from signals entering through P0 and P1 ports. These last two signals (those that enter P0 and P1 ports) are digital and come out from the PC (Fig. 1). The 10 MHz shifted signal is then mixed with the signal at BASEBAND SIGNAL INPUT port (it may be gaussian, square, or sinc) that comes from the PCI-766 pulse generator card (PGC from Fig. 1). This resulting signal is mixed again with the 74 MHz signal at RF 2 INPUT port and finally amplified and filtered by the PASSBAND FILTER module in order to obtain the modulated 64 MHz signal. The 74 MHz signal is attenuated by the RF SWITCH when there is no baseband signal present, thus reducing noise and unwanted effects at the output of the modulator. The RF SWITCH module is controlled by the RF SWITCH CONTROL module control circuit, which is commanded by the RF ON/OFF signal coming out from the PC (Fig. 1). The modulator has 0 dBm nominal input power and 256 output levels (up to 3 dBm).

2.1.2- VERIFYING THE FREQUENCY RANGE OF THE COMPONENTS

The main components of the old modulator, their correspondent frequency range and the frequency in which they must work for the upgraded modulator are shown in Table 1:

Table 1
Components' frequency range and working frequency

Component	Frequency range (MHz)	Working frequency (MHz)
PHASE SHIFTER (combinations of PSJ-2-1, see [21])	1-200	10
MIXER 1 (GRA-3, see [21])	DC-200	10
MIXER 2 (GRA-3, see [21])	DC-200	10, 74, 64
RF SWITCH (PAS-3, see [21])	DC-2000	74
PREAMPLIFIER (MAV-11, see [21])	DC-1000	64
PASSBAND FILTER (Already designed)	DC-4	64

As can be observed, all the components from the old modulator can work well at the 64 MHz frequency, except for the passband filter, which needs to be redesigned and rebuilt for working at 64 MHz.

2.1.3- CHECKING THE PERFORMANCE OF THE RF SWITCH

The signal output from the modulator is necessary only when exciting the substance under study; therefore, it needs to be suppressed or attenuated during the reception process. This suppression was carried out using the PAS-3 part in the old

modulator as shown in Table 1, but in the upgraded version, with the rising of the working frequency up to 64 MHz this component was not good enough to achieve this function and a new RF switch was used: the KSWHA-1.20 [21]. This new RF switch has a 69 dB isolation from the input to the output port when turned off and 0,75 dB insertion loss when turned on, all this for 64 MHz and at RF level of 0 dBm.

The new switch requires certain control signals and the electronics necessary to control this switch with the right signal levels was designed and built by the authors of this work. There are two pins to control this switch: to turn it on, a 0 V is required on a pin and a -8 V is needed on the other one, and to turn it off, the voltages must be interchanged. The control circuit for the RF switch is shown in Fig. 3. This control circuit is driven by a TTL signal coming from the PC and at its output there are two signals: 0 V and -8 V on each terminal and interchangeable when needed that allows to activate or not the RF switch.

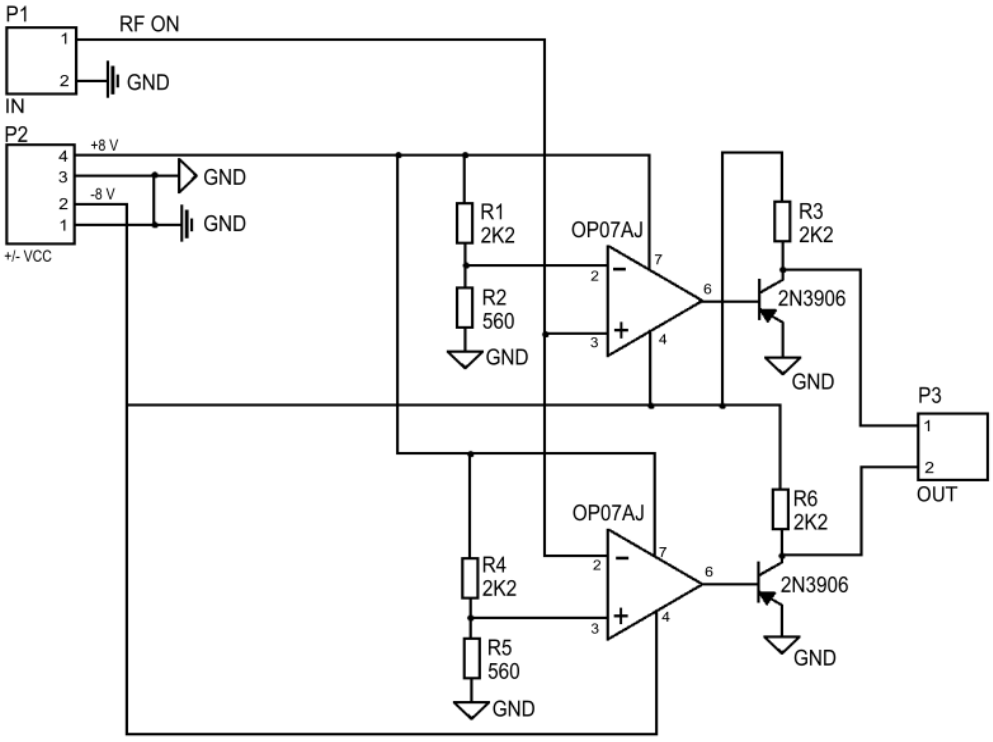

Figure 3

Schematic diagram of RF switch control circuit.

2.1.4- THE OUTPUT FILTER OF THE MODULATOR

The signal from the modulator is sent to the output through a passband filter centered around 64 MHz that was designed and built by the authors of this work. This filter was designed to have cut off frequencies at 60 MHz and 70 MHz respectively and a bandwidth of 10 MHz. It was also designed to be coupled to 50 Ω.

The designed filter is of type π and its schematic is shown in Fig. 4.

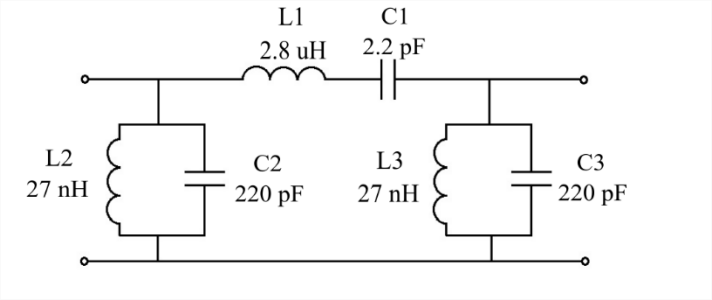

Figure 4

64 MHz passband filter of type π with commercial component values.

The component values are calculated through the following expressions [22]

$$L_{1k} = \frac{R}{\pi(f_2 - f_1)} \tag{2}$$

$$L_{2k} = \frac{(f_2 - f_1)R}{4\pi f_1 f_2} \tag{3}$$

$$C_{1k} = \frac{f_2 - f_1}{4\pi f_1 f_2 R} \tag{4}$$

$$C_{2k} = \frac{1}{\pi(f_2 - f_1)R} \tag{5}$$

$$L_1 = L_{1k} \tag{6}$$

$$L_2 = L_3 = 2L_{2k} \tag{7}$$

$$C_1 = C_{1k} \tag{8}$$

$$C_2 = C_3 = \frac{C_{2k}}{2} \tag{9}$$

Where: f_1 is the passband lower frequency limit, and is equal to 60 MHz.

f_2 is the passband higher frequency limit, and is equal to 70 MHz.

R is the load resistance, and is equal to 50 Ω.

$L_{1k}, L_{2k}, C_{1k}, C_{2k}$ are intermediate results.

$L_1, L_2, L_3, C_1, C_2, C_3$ are the final values of the components.

Once the components were calculated, the commercial values were selected as shown in Fig. 4.

3.- RESULTS AND DISCUSSION

With all these changes made to the modulator, a validation process was carried out. First, the theoretical and practical frequency response of the filter alone was determined because its frequency response is important to the system; second, the

correct performance of the modulator is measured; and finally, the correct performance of the spectrometer with the upgraded modulator fitted into is tested.

The two frequency characteristics of the design and implemented filter are shown in Fig. 5, the black line being the ideal response of the designed filter on software, and the red one, the practical response. The 3 dB frequencies of the real filter, 60 MHz and 70 MHz, have an attenuation of 20 dB and 15 dB with respect to the ideal response. There are three vertical lines in Fig. 5: at 54 MHz, 64 MHz and 74 MHz respectively. The 54 MHz and 74 MHz frequencies were selected because they arise in the process of mixing and are very close to the filter bandwidth (this is not desired) as will be calculated later, and need to be attenuated. At 64 MHz there is an attenuation of the real response with respect to the ideal one of about 19 dB, and of 13 dB with respect to 0 dB. At 54 MHz there is an attenuation of the real response with respect to the ideal one of 16 dB, and of 48 dB with respect to 0 dB. At 74 MHz there is an attenuation of the real response with respect to the ideal one of 16 dB, and of 30 dB with respect to 0 dB.

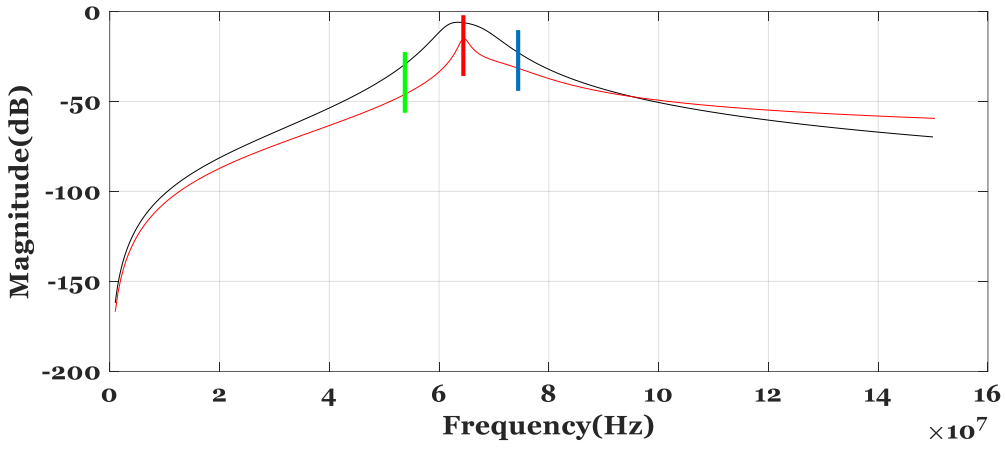

Figure 5

Frequency responses of the software designed (black line) and practical (red line) output filter with line markers at 54 MHz (green), 64 MHz (red) and 74 MHz (blue).

To verify the correct performance of the modulator, the signals entering its ports were set up as follows: Three signals were provided to the BASEBAND SIGNAL INPUT port in Fig. 2 one at a time (gaussian, square, sinc), and each one had a 1 mV peak-to-peak amplitude and a 0.2 ms length. The signals at the RF 1 INPUT and RF 2 INPUT ports in Fig. 2 were sinusoidal signals of 10 MHz and 1 V peak to peak, and 74 MHz and 1 V peak to peak, respectively. The 64 MHz output signal obtained from the modulator was captured and digitized with a digital oscilloscope and further processed using the FFT in order to find the characteristic parameters of the modulator such as: harmonic suppression, sideband rejection and conversion loss.

Figs. 6, 7 and 8 show the measured signals and their spectra at the output of the modulator for the three pulses used: gaussian, square and sinc, respectively. In Figs. 6 a), 7 a) and 8 a), the envelope of the output signals can be observed. The important fraction of the signals in Figs. 6 a), 7 a) and 8 a) lies between 0.18 ms and 0.38 ms approximately, because it is in this interval that the baseband signal modulates the carrier, but the RF switch is turned on and allows the signal from the modulator to go out from 0.07 ms to 0.48 ms. The RF switch is turned on before the modulation process for the proper functioning of the modulator, because there is a delay to wait until the baseband signals and the other RF signals go through the electrical components of the modulator and finally get mixed and go out of the modulator. In the interval from 0 to 0.18 ms and from 0.48 ms onwards approximately, the signal is highly attenuated because the RF switch is turned off. This demonstrates the good performance of the RF switch and allows the modulator to work well.

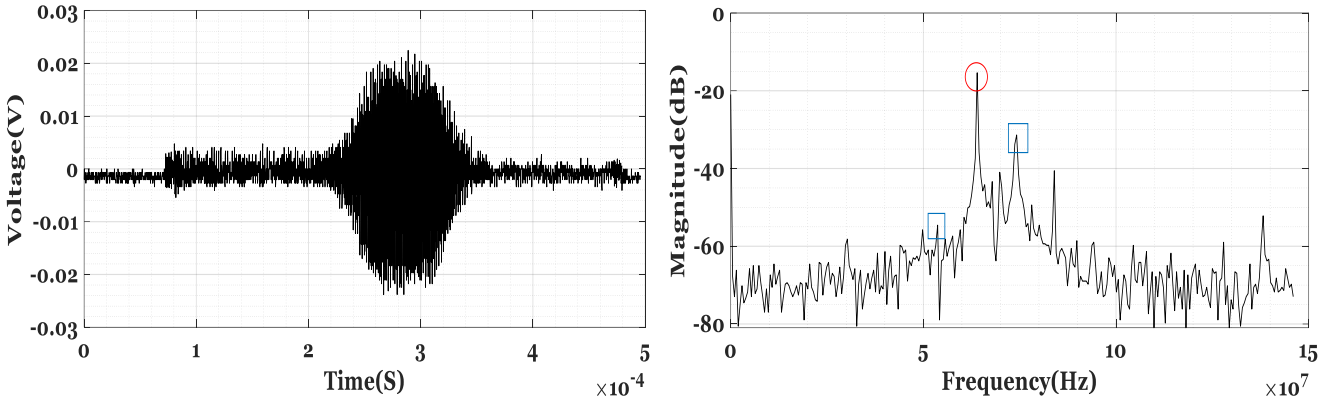

a) b)

Figure 6

Characteristic of the signal at the output of the modulator using a gaussian waveform as the modulating signal. a) Time signal b) Frequency spectrum with red circle at 64 MHz and blue squares at 54 MHz and 74 MHz.

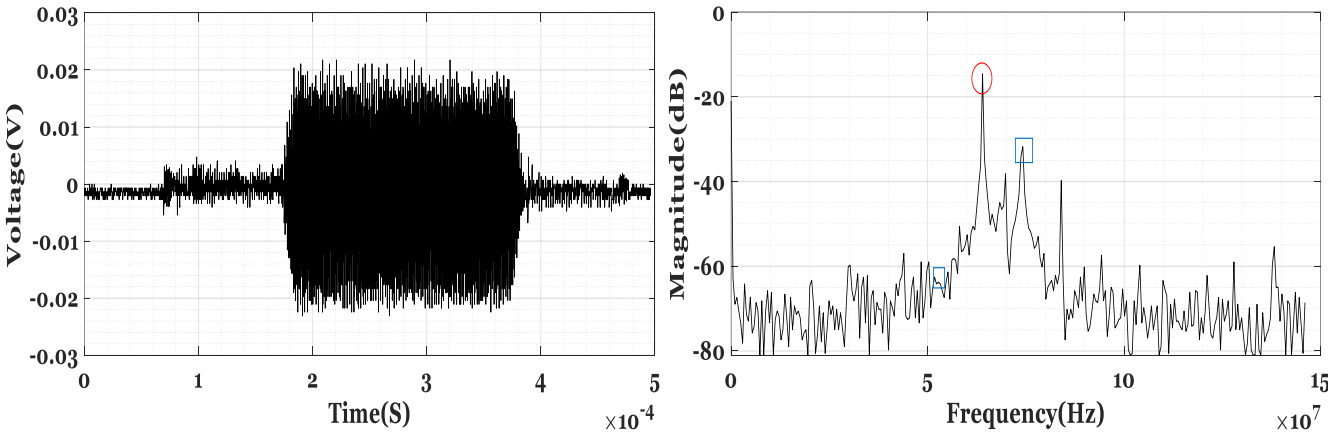

a) b)

Figure 7

Characteristic of the signal at the output of the modulator using a square waveform as the modulating signal. a) Time signal b) Frequency spectrum with red circle at 64 MHz and blue squares at 54 MHz and 74 MHz.

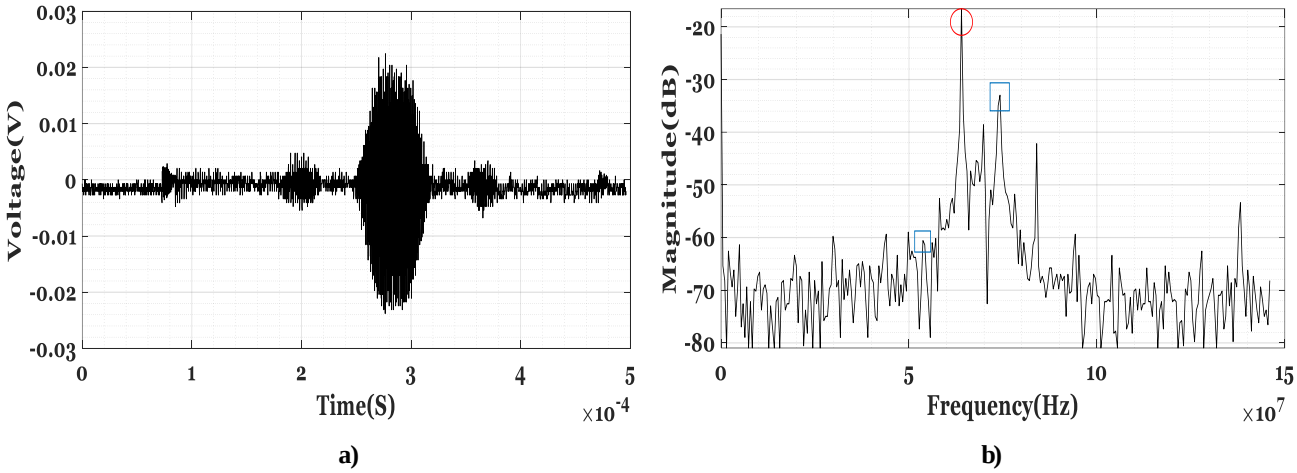

Figure 8

Characteristic of the signal at the output of the modulator using a sinc waveform as the modulating signal. a) Time signal b) Frequency spectrum with red circle at 64 MHz and blue squares at 54 MHz and 74 MHz.

In 6 b), 7 b) and 8 b) it can be observed that the highest power frequency component (highest level marked with a red circle) is always at 64 MHz, which corresponds to the desired frequency output and is attenuated due to the characteristic of the output filter at this frequency. The 54 MHz and 74 MHz frequencies (levels marked with a blue square) are present at the output and attenuated by the filter. For a detailed evaluation of the modulator performance, harmonic suppression, sideband rejection and conversion loss are measured and calculated from the data plotted in Fig. 6 b), 7 b) and 8 b), taking into account the main frequencies at the output of the modulator and others resulting from the mixing process.

The most important harmonics in the modulation process are the 3rd and the 5th because they are the closest to the working frequency [21]. The measured harmonic suppressions of the 3rd and 5th orders are shown in Table 2: The measured harmonics were the sum and difference between the carrier and the products of the intermediate frequency (64 MHz + or - n*10 MHz, with n being 3 and 5).

Table 2
Harmonic suppression

Harmonics	Orders	Levels (dB)			Suppressions (dB)		
		Gaussian	Square	Sinc	Gaussian	Square	Sinc
94 MHz	3rd (64 MHz+3*10 MHz)	-59	-57	-59	44	43	43
114 MHz	5th (64 MHz+5*10 MHz)	-62	-74	-72	47	60	56
34 MHz	3rd (64 MHz-3*10 MHz)	-76	-73	-66	61	59	50
14 MHz	5th (64 MHz-5*10 MHz)	-70	-72	-80	55	58	64

As it can be observed, all the suppression levels are equal to or greater than 40 dB, which ensures good harmonic attenuation and a cleaner signal, limiting the possibility of exciting the probe at other frequencies.

When measuring sideband rejection, there were two important frequencies near the 64 MHz frequency (this was the important frequency) which needed to be measured and were the result of the mixing process of the intermediate frequency (10 MHz) and 64 MHz; these frequencies were 54 MHz and 74 MHz. Rejection values are shown in Table 3.

Table 3
Sideband rejection

Frecuencies	Rejection (dB)		
	Gaussian	Square	Sinc
74 MHz (64 MHz+10 MHz)	20	17	17
54 MHz (64 MHz –10 MHz)	40	52	45

The minimum rejection of the 74 MHz frequency is 17 dB. It is low, but it does not affect the experiment because the probehead is tuned to 64 MHz and further attenuates the unwanted frequency of 74 MHz. The minimum rejection of the 54 MHz frequency is 40 dB.

The conversion loss of the modulator was measured taking into account the two RF inputs of the modulator and the RF output. Conversion loss was approximately 20 db. It is a high conversion loss, and the cause of this loss is the filtering stage. This loss was corrected by introducing an RF power amplifier after the modulator.

Finally, to validate the correct performance of the spectrometer, the upgraded modulator was fitted into to the spectrometer and a real acquisition of an NMR signal was carried out.

To carry out this experiment, a sample of choline was dissolved in H_2O. Its NMR signal and spectrum are shown in Fig. 9. The NMR signal shown in Fig. 9 a) corresponds to one acquisition without accumulations and it is obtained with 256 time points and with a sampling frequency of 1.3 kHz. From Fig. 9 b) it is observed that the choline has a characteristic spectrum with a main singlet resonance at 3.18 ppm, and water has a characteristic spectrum at 4.7 ppm, with the chemical shift (ppm) relative to DSS (2,2-dimethyl-2-silapentane-5-sulfonate), with both resonances visible in Fig. 9 b). Choline has a couple of additional resonances at 4.05 ppm and 3.5 ppm, but their amplitude relative to the main resonance are too small to be observed in the spectrum [23].

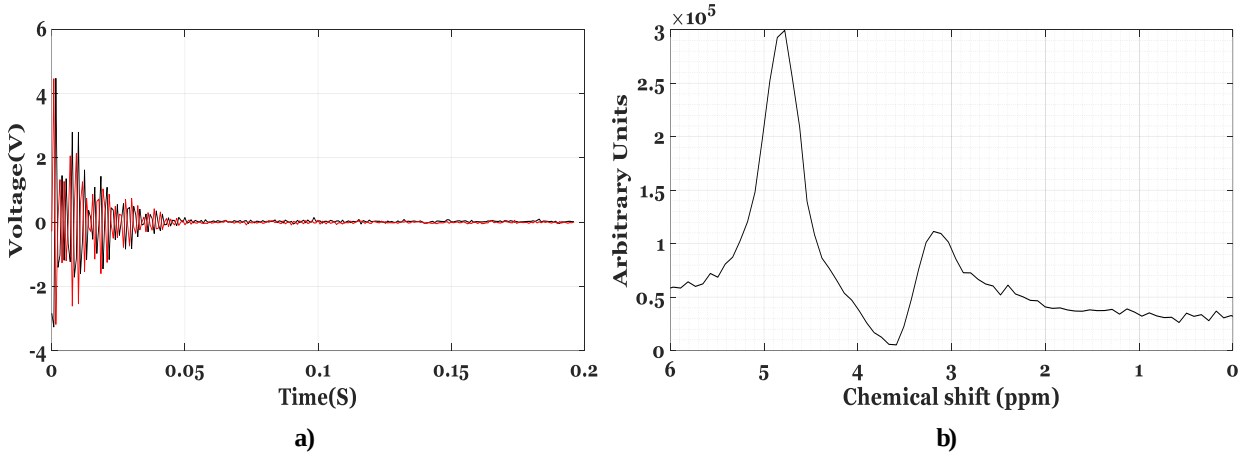

Figure 9

RMN signal and spectrum of choline dissolved in H_2O obtained at the spectrometer. a) Real (red) and Imaginary (black) signals b) Spectrum.

4.- CONCLUSIONS

Upgrading the modulator made it possible for the spectrometer to work properly, providing the latter with the new functionality to operate at the 64 MHz frequency; and thus, to carry out experiments at 1.5 T. This field is very common in MRI clinical machines; therefore, the spectrometer may be used to analyse substances and compare the results with those of other studies conducted on 1.5 T MRI machines.

This paper demonstrates that it is possible to upgrade the RF modulator for different frequencies, depending on the desired applications; as long as it is a modular design. This upgrading was accomplished at a low cost, with common electronic components, and within a reasonable time interval.

The upgrading of the RF modulator, which constitutes an electronically open system, allows conducting research in the fields of biotechnology, medicine and others, and could become an experimental and teaching basis for learning in NMR technology.

REFERENCES

1. Lambert JB, Mazzola EP, Ridge CD. Nuclear magnetic resonance spectroscopy: an introduction to principles, applications, and experimental methods: Wiley; 2019.
2. Powers R. The current state of drug discovery and a potential role for NMR metabolomics: miniperspective. Journal of medicinal chemistry. 2014;57(14):5860-70.
3. Wen H, An YJ, Xu WJ, Kang KW, Park S. Real-time monitoring of cancer cell metabolism and effects of an anticancer agent using 2D in-cell NMR spectroscopy. Angewandte Chemie International Edition. 2015;54(18):5374-7.
4. Jakes W, Gerdova A, Defernez M, Watson A, McCallum C, Limer E, et al. Authentication of beef versus horse meat using 60 MHz 1H NMR spectroscopy. Food Chemistry. 2015;175:1-9.
5. Haouas M, Taulelle F, Martineau C. Recent advances in application of 27Al NMR spectroscopy to materials science. Progress in nuclear magnetic resonance spectroscopy. 2016;94:11-36.
6. Fan TW-M, Lane AN. Applications of NMR spectroscopy to systems biochemistry. Progress in nuclear magnetic resonance spectroscopy. 2016;92:18-53.
7. Hoult DI, Richards R. The signal-to-noise ratio of the nuclear magnetic resonance experiment. Journal of Magnetic Resonance (1969). 1976;24(1):71-85.
8. Quinn CM, Wang M, Polenova T. NMR of macromolecular assemblies and machines at 1 GHz and beyond: new transformative opportunities for molecular structural biology. Protein NMR: Springer; 2018. p. 1-35.
9. Brown RW, Cheng Y-CN, Haacke EM, Thompson MR, Venkatesan R. Magnetic resonance imaging: physical principles and sequence design. 2014.
10. Moser E, Laistler E, Schmitt F, Kontaxis G. Ultra-high field NMR and MRI—The role of magnet technology to increase sensitivity and specificity. Frontiers in Physics. 2017;5:33.
11. Chen Z, Cai S, Huang Y, Lin Y. High-resolution NMR spectroscopy in inhomogeneous fields. Progress in nuclear magnetic resonance spectroscopy. 2015;90:1-31.
12. Kuzmin V, Bogaychuk A, Nekrasov I, Safiullin K, Salakhov M, Alakshin E, et al. The home-built high-field multifunctional pulsed NMR spectrometer. Magnetic Resonance in Solids Electronic Journal. 2019;21(1).
13. Zalesskiy SS, Danieli E, Blumich B, Ananikov VP. Miniaturization of NMR systems: Desktop spectrometers, microcoil spectroscopy, and "NMR on a chip" for chemistry, biochemistry, and industry. Chemical reviews. 2014;114(11):5641-94.
14. Pandey MK, Zhang R, Hashi K, Ohki S, Nishijima G, Matsumoto S, et al. 1020 MHz single-channel proton fast magic angle spinning solid-state NMR spectroscopy. Journal of Magnetic Resonance. 2015;261:1-5.
15. Schwalbe H. New 1.2 GHz NMR Spectrometers—New horizons? Angewandte Chemie International Edition. 2017;56(35):10252-3.
16. Ha D, Sun N, Paulsen J, Song Y, Tang Y, Hong S, et al., editors. Integrated CMOS spectrometer for multi-dimensional NMR spectroscopy. 2017 IEEE 60th International Midwest Symposium on Circuits and Systems (MWSCAS); 2017: IEEE.
17. Cousin SF, Charlier C, Kadeřávek P, Marquardsen T, Tyburn J-M, Bovier P-A, et al. High-resolution two-field nuclear magnetic resonance spectroscopy. Physical Chemistry Chemical Physics. 2016;18(48):33187-94.
18. Phuc HD. Development of portable low field NMR magnet: Design and construction 2015.
19. Webber JBW, Demin P. Credit-card sized field and benchtop NMR relaxometers using field programmable gate arrays. Magnetic resonance imaging. 2019;56:45-51.
20. Louis-Joseph A, Lesot P. Designing and building a low-cost portable FT-NMR spectrometer in 2019: A modern challenge. Comptes Rendus Chimie. 2019.
21. Minicircuits. Minicircuits Products; 2017. Available from: https://www.minicircuits.com/.
22. Gray L, Graham R. Radio transmitter: McGraw-Hill; 1961.
23. Govindaraju V, Young K, Maudsley AA. Proton NMR chemical shifts and coupling constants for brain metabolites. NMR in Biomedicine. 2000;13:129-153.

CONFLICT OF INTERESTS

None of the authors stated the existence of possible conflicts of interest that should be declared in relation to this article.

CONTRIBUTIONS OF THE AUTHORS

Joaquin Enrique Hing Batista: He made an important contribution to the electronic upgrade of the modulator, its assembly and performance evaluation. He carried out the bibliographic review, its analysis and interpretation. He drafted the article and its final version.

Alejandro Bordelois Boizán: He made a contribution in the stage of preparation of the experiment for the acquisition of the NMR signal. He contributed to the literature review. He participated in the article drafting, critical review of the final version and approval.

Manuel Ernesto Noda Guerra: He made a contribution in the measurement of the modulator parameters and the NMR signal of the spectrometer. He contributed to the literature review. He participated in the critical review of the draft and the approval of the final version of the article to be published.

AUTHORS

Joaquin Enrique Hing Batista, Telecommunications and Electronics Engineer, graduated from the Universidad de Oriente, Santiago de Cuba, Cuba, in 2014. He works at the Centro de Biofísica Médica. Email: joaquin.hing@gmail.com .ORCID number: https://orcid.org/0000-0001-9449-2410. His research interests include Magnetic Resonance systems and signal processing.

Alejandro Bordelois Boizán, Ph.D. degree from the University of Rennes 1, Rennes, France, in 2013. Since 2006, he works at the Centro de Biofisica Médica of the Universidad de Oriente, Cuba. Email: borde268@gmail.com .ORCID number: https://orcid.org/0000-0001-9978-6151. His research interests include the design of magnets, gradient and shimming coils for low field MRI applications and MR spectroscopy.

Manuel Ernesto Noda Guerra, Bachelor of Science in Physics, graduated from the Universidad de Oriente, Santiago de Cuba, Cuba, in 1990. He works at the Centro de Biofísica Médica. Email: man.noda@gmail.com. ORCID number: https://orcid.org/0000-0002-3837-2112. His research interests include Magnetic Resonance (MR) systems and signal processing.